

Carsten Ehrhardt · Carsten Kneuer · Jennifer Fiegel  
Justin Hanes · Ulrich Friedrich Schaefer  
Kwang-Jin Kim · Claus-Michael Lehr

## Influence of apical fluid volume on the development of functional intercellular junctions in the human epithelial cell line *16HBE14o-*: implications for the use of this cell line as an in vitro model for bronchial drug absorption studies

Received: 24 August 2001 / Accepted: 13 February 2002 / Published online: 27 April 2002  
© Springer-Verlag 2002

**Abstract** Air-interfaced culture (AIC) versus liquid-covered culture (LCC) conditions are known to have different effects on the differentiated phenotype of several cell types, including lung epithelial cells. We report the influence of culture conditions such as apical medium volume on the development of intercellular junctions in the human epithelial cell line *16HBE14o-*. Immunofluorescence staining of the tight-junctional protein, ZO-1, has revealed its presence in cells grown in both AIC and LCC. However, only LCC-grown cells exhibit protein ZO-1 localized as a zonula-occludens-like regular belt connecting neighboring cells. The presence of typical tight junctions has been confirmed by electron microscopy. Immunostaining for occludin, claudin-1, connexin43, and E-cadherin has demonstrated intercellular junction

structures only in the cells in LCC. These morphological findings have been paralleled by higher transepithelial electrical resistance values and similar fluxes of the hydrophilic permeability marker, fluorescein-Na, under LCC compared with AIC conditions. We conclude that the formation of functional *16HBE14o-* cell layers requires the presence of an apical fluid volume, in contrast to other culture conditions for airway epithelial cells.

**Keywords** Air-interface · E-cadherin · Occludin · Claudin-1 · ZO-1 · Connexin · Intercellular junctions · Human epithelial cell line (*16HBE14o-*)

This work was supported in part by the ZEBET (C.E., U.F.S., C.M.L. WK 1-1328-152), the National Science Foundation (J.F. and J.H., grant DGE-9616062), the Whitaker Foundation (J.F. and J.H., grant RG-99-0046), research grants from the National Institutes of Health (K.J.K., HL 38658, HL 64365) and a Grant-in-Aid (K.J.K., 990542 N) from the American Heart Association

C. Ehrhardt · C. Kneuer · U.F. Schaefer · C.-M. Lehr (✉)  
Department of Biopharmaceutics and Pharmaceutical Technology,  
Bldg. 8.1, Saarland University, 66123 Saarbrücken, Germany  
e-mail: lehr@mx.uni-saarland.de  
Tel.: +49-681-3022039, Fax: +49-681-3024677

J. Fiegel · J. Hanes  
Department of Chemical Engineering, Johns Hopkins University,  
Baltimore, MD 21218, USA

J. Hanes  
Department of Biomedical Engineering,  
Johns Hopkins University, Baltimore, MD 21205, USA

K.-J. Kim  
Will Rogers Institute Pulmonary Research Center,  
Division of Pulmonary and Critical Care Medicine,  
Departments of Medicine, Physiology and Biophysics,  
Biomedical Engineering,  
and Molecular Pharmacology and Toxicology,  
University of Southern California, Los Angeles, CA 90033, USA

### Introduction

Over the last few years, considerable efforts have been made to develop reliable in vitro models that allow a mechanistic examination of cellular and molecular processes involved in the absorption and metabolism of xenobiotic drugs. In addition to the gastrointestinal tract, to which much attention has been given, the pulmonary region has recently become an attractive site for drug delivery research. In this context, protocols have been developed for the isolation and cultivation of primary respiratory epithelial cells, either of human or animal origin (Cheek et al. 1989; Dobbs 1990; Elbert et al. 1999; Shen et al. 1999). Additionally, cancer cell lines have been screened for their suitability to serve as in vitro models (Artursson 1990; Shen et al. 1994), and new airway epithelial cell lines, which preserve the differentiated phenotype, have been obtained by immortalization (Cozens et al. 1992, 1994).

The cell line *16HBE14o-* has been generated by the transformation of normal human bronchial epithelial cells (Cozens et al. 1994). The cell line affords easy maintenance and avoids several difficulties including reproducibility and high costs associated with primary cul-

ture approaches. The *16HBE14o-* cells retain differentiated epithelial morphology by forming polarized cell layers with microvilli and cilia; both the mRNA and protein for the cystic fibrosis transmembrane conductance regulator are present, and the cells stain positively with antibodies against cytokeratin and E-cadherin (old name: cell adhesion molecule 120/80, abbreviated to cellCAM 120/80; Cozens et al. 1994). It has been reported (Zhu et al. 1999) that the expression levels for intercellular adhesion molecule 1 (ICAM-1) are similar for *16HBE14o-* cells and explanted bronchial epithelial cells. Messenger RNAs encoding epidermal growth factor receptor, c-erbB2, and c-erbB3 have been detected in both primary cultures of human bronchial epithelial cells and *16HBE14o-* cells (Polosa et al. 1999). *16HBE14o-* cell layers are also known to bind lectins specific to bronchial epithelial cells (Dorscheid et al. 1999). Because of its well-conserved phenotype, the *16HBE14o-* cell line has been used to study various physiological and pathological processes, such as inflammation, infection, and cytokine expression (Salvi et al. 1999; Bonvallot et al. 2001; Hodge et al. 2001; Aoki et al. 1998; Man et al. 2000). To our knowledge, the feasibility of using the *16HBE14o-* cell line for studying the transport of pharmaceutically relevant substances across the bronchial epithelium has not been reported.

The choice of culture conditions is known to be highly relevant for the proliferation and differentiation of cells. In addition to the choice of culture medium, substratum coating, and cell-seeding density, the volumes of media on each side of the epithelial barrier may be crucial. For airway epithelial cells, which are directly exposed to air *in vivo*, the air-interfaced culture has been found to yield a well-differentiated phenotype (Yamaya et al. 1992; Mathias et al. 1995). This idea has also been applied successfully to *in vitro* models of the conjunctival epithelium (Yang et al. 2000) and skin equivalents (Mak et al. 1991). Yamaya et al. (1992) have demonstrated that the differentiation of human tracheal epithelial cells in culture is inversely correlated to the depth of liquid overlying the apical surface of the cells.

For the characterization of an *in vitro* model for drug absorption, it is crucial that the cell layer presents a functional barrier, similar to that of epithelial tissue *in vivo*. Therefore, information about the influence of culture conditions on the formation of cellular junctions is of great importance. The connections between adjacent cells are complex, and fundamental knowledge has been accumulated concerning the morphology and physiology of cellular junctions during the last decade.

Tight junctions constitute the principal barrier to the passive movement of fluid, electrolytes, macromolecules, and blood-borne cells through the paracellular pathway and specifically contribute to the transepithelial transport of compounds (e.g.,  $Mg^{2+}$ ; Simon et al. 1999). Proteins that are involved in the formation of tight junctions include the transmembrane proteins, occludins, and claudins (Furuse et al. 1994, 1998; Morita et al. 1999). The intracellular proteins related to tight-junctional func-

tions are the zonula occludens proteins ZO-1, ZO-2, and ZO-3 (Itoh et al. 1999), which belong to the membrane-associated guanylate kinase (MAGUK) family of proteins. ZO-1 has been found to be associated with occludin and appears to link it to the actin-based cytoskeleton (Fanning et al. 1998). Other tight-junction-related proteins involved in this process include ZO-2, ZO-3, cingulin, 7H6 antigen, and symplekin (Mitic and Anderson 1998). The formation of the zonula occludens in epithelia is known to be accompanied by that of the zonula adherens. The interface of the actin-myosin II ring with the lateral membrane can be localized at this level. The type I membrane protein, E-cadherin, which connects two neighboring cells by  $Ca^{2+}$ -dependent interactions, is also located here. The actin-myosin II filament aligned within the ring allows for contraction of the assembly (Madara 1987). Gap-junctional intercellular communication (GJIC) might be regulated by  $Ca^{2+}$ -dependent CAMs, such as E-cadherin, and the alteration of GJIC via CAM may be involved in carcinogenesis (Jinn 1998). Thus, crosstalk between gap junctions and adherens junctions appears to occur (Lampe and Lau 2000). The channel-forming connexons are composed of subunit proteins encoded by the multigene connexin family. More than 20 members have been identified and show a wide variability in their tissue distribution (Simon and Goodenough 1998). Connexin43 (Cx43) is ubiquitously expressed in normal tissue of the airways (Abraham et al. 2001; Ruch et al. 2001).

In this study, we have investigated the influence of various apical medium volumes on the expression of the main proteins related to the cellular junctions and the cytoskeletal organization in the cell line *16HBE14o-* in order to find the optimal culture conditions for retaining a robust model for studies of drug delivery to the bronchial region of the lung.

---

## Materials and methods

### Cells and culture conditions

The *16HBE14o-* cells were a gift from Dr. Dieter C. Gruenert (Cardiovascular Research Institute at the University of California, San Francisco, Calif., USA). This continuous cell line was generated by transformation of normal bronchial epithelial cells obtained from a 1-year-old heart-lung transplant patient. Transformation was accomplished with SV40 large T antigen by using the replication defective pSVori<sup>-</sup> plasmid. Passages 2.47 to 2.78 were used in this study. Cells were seeded onto Transwell Clear permeable filter inserts (12 mm in diameter with a pore size of 0.4  $\mu$ m; Corning, Wiesbaden, Germany) at a density of  $10^5$  cells/cm<sup>2</sup> and grown in Eagle's minimum essential medium supplemented with 10% fetal calf serum, 0.1 mM non-essential amino acids, 2 mM L-glutamine, 100  $\mu$ g/ml streptomycin, and 100 U/ml penicillin G, at 37°C in a 5% CO<sub>2</sub> incubator. Starting on day 1, i.e., 24 h after seeding, the volumes of the apical and basolateral chambers were set as follows. For cells grown in liquid-covered culture (LCC), the apical/basolateral fluid volumes were: 1000  $\mu$ l/2100  $\mu$ l, 750  $\mu$ l/1800  $\mu$ l, 500  $\mu$ l/1500  $\mu$ l, 250  $\mu$ l/900  $\mu$ l, or 100  $\mu$ l/750  $\mu$ l. These volume pairs were chosen to avoid any significant hydrostatic pressure gradient across the cell layers. For cells cultured under air-interfaced culture (AIC) conditions, the apical medium

was removed, and the volume on the basolateral side was replenished to 700  $\mu$ l. The culture medium was changed daily. Preliminary studies showed no significant influence of coating of the filters either with fibronectin/collagen or Vitrogen-100 on the trans-epithelial electrical resistance (TEER) over 21 days in culture (data not shown). By employing TEER measurements and light microscopy, the optimal seeding density was determined to be  $10^5$  cells/cm<sup>2</sup>. To assure the quality of the cell line, immunocytochemical staining studies were performed. Antibodies against the epithelial marker cytokeratin 18 and the lung-specific prosurfactant protein C were used, revealing that more than 99% of cells were positive for both markers by fluorescence-activated cell-sorting analysis (data not shown). All chemicals were obtained from Sigma (Deisenhofen, Germany) unless noted otherwise.

#### Bioelectric measurements

The time for the cellular layer to reach confluence was determined by measuring the TEER as a function of the days in culture. TEER was measured daily with an epithelial volt-ohm-meter equipped with STX2 "chopstick" electrodes (WPI, Berlin, Germany) and corrected for the background value contributed by the Transwell Clear filter and medium. Appropriate volumes of pre-warmed medium were added to the apical and basolateral sides of Transwell-grown cell layers residing in wells containing less than the standard (500  $\mu$ l apical/1500  $\mu$ l basolateral) volumes of fluid. Cell layers were then allowed to equilibrate for 10 min prior to TEER measurement. The assessment of TEER values was performed with cells cultured from at least three different passages to ascertain reproducibility.

#### Immunocytochemical staining

Mouse monoclonal Cx43 antibody and rabbit polyclonal antibodies to ZO-1 and claudin-1 were obtained from Zymed (South San Francisco, USA); mouse monoclonal IgG1 antibodies to occludin and E-cadherin were from BD Transduction Laboratories (Heidelberg, Germany). Actin was stained with phalloidin labeled with tetramethylrhodamine isothiocyanate (Sigma). All antibodies were diluted 1:100 in phosphate-buffered saline (PBS) plus 1% bovine serum albumin (BSA) at pH 7.2, and phalloidin was used at a concentration of 500 ng/ml. Mouse IgG1 $\kappa$  (Sigma) was used as an isotypic control. Cell layers were stained for ZO-1 at 2 days, 4 days, 1 week, and 2 weeks after seeding and for occludin, claudin-1, Cx43, E-cadherin, and actin after 1 week in culture. Cells were prepared for staining by a 10-min fixation in 2% paraformaldehyde and a 10-min blocking step in 50 mM NH<sub>4</sub>Cl, followed by permeabilization for 8 min with 0.1% Triton X-100. After a 60-min incubation with a primary antibody, the cell layers were washed at least three times with PBS before being reacted with a 1:100 dilution of a fluorescein isothiocyanate (FITC)-labeled goat anti-mouse F(ab')<sub>2</sub> fragment or swine anti-rabbit F(ab')<sub>2</sub> fragment (DAKO, Hamburg, Germany) in PBS plus 1% BSA. Propidium iodide (1  $\mu$ g/ml) was added for the counterstaining of cell nuclei. After 30 min incubation, the samples were washed again three times with PBS and embedded in FluorSave anti-fade medium (Calbiochem, Bad Soden, Germany). Images were obtained by a confocal laser scanning microscope (MRC-1024, bio-rad, Munich, Germany) with the instrument settings adjusted so that no positive signal was observed in the channel corresponding to green fluorescence for the isotypic controls.

#### Transport studies

Transport experiments with the model compound fluorescein-Na (Flu-Na, MW: 376.3 Daltons) were carried out on day 2, days 4–9, and day 18 in culture. Further transport experiments were performed with cell layers cultured for 1 week by using FITC-labeled dextran (4 kDa, FD4) and two drugs belonging to the biopharma-

ceutics classification systems (BCS; Amidon et al. 1995), viz., the lipophilic propranolol (Pro) and the hydrophilic atenolol (Ate). All experiments were conducted in freshly prepared bicarbonate-buffered Krebs Ringer (KRB, pH 7.4: 116.4 mM NaCl, 5.4 mM KCl, 0.78 mM NaH<sub>2</sub>PO<sub>4</sub>, 25 mM NaHCO<sub>3</sub>, 1.8 mM CaCl<sub>2</sub>, 0.81 mM MgSO<sub>4</sub>, 15.0 mM HEPES, and 5.55 mM glucose). Both sides of the cultured cell layers were washed twice with KRB. The washed cell layers were then placed in new cluster plates containing 1.5 ml KRB per well (representing the receiver compartment) prewarmed to 37°C. After a 60-min equilibration, experiments were initiated by replacing the buffer in the apical donor chamber with 0.52 ml 50  $\mu$ M (final concentration) each of Flu-Na, FD4, and Pro solution in KRB. Ate was used at a final concentration of 500  $\mu$ M. The initial concentration in the donor fluid was assayed by taking a 20- $\mu$ l sample directly after adding the drug solution. The cell layers were agitated by an orbital shaker at a constant stirring rate (100 rpm) at 37°C during transport experiments. Samples of 200  $\mu$ l each were serially drawn from the receiver compartment at 0.5, 1, 2, 3, and 4 h. To maintain sink-conditions, the cell layers on Transwell Clear filters were placed in fresh wells containing 1.5 ml pre-warmed KRB after each sampling. At the end of the experiment, another 20- $\mu$ l sample was drawn from the donor compartment and assayed for its activity. Each experiment was performed in triplicate. In order to assess the integrity of a cell layer during the flux experiment, TEER was measured before and after each transport experiment.

Flux ( $J$ ) was determined by plotting the cumulative amounts of drug traversed across the cell layers versus time. Apparent permeability coefficients,  $P_{app}$ , were calculated according to the equation  $P_{app} = J/(A \cdot C_i)$ , where  $C_i$  is the initial concentration of the given drugs in the donor fluid, and  $A$  the surface area of the filter (1.13 cm<sup>2</sup>) utilized in this study. The fluorescence of the samples (Flu-Na and FD4) was analyzed in 96-well plates by using a fluorescence plate reader (Cytofluor II, PerSeptive Biosystems, Wiesbaden, Germany) at excitation and emission wavelengths of 485 nm and 530 nm, respectively. Ate and Pro were analyzed by reversed phase/high pressure liquid chromatography on a Dionex Summit System equipped with a P580 pump, ASI100 automated sampler, and UVD170S UV/VIS detector (Dionex, Idstein, Germany). Chromatograms were analyzed by means of peak area calculation by using a computerized data integration program (Chromleon 6.1, Dionex). Samples were diluted with KRB, where appropriate.

#### Electron microscopy

*16HBE14o-* cell layers cultured on Transwell filters were washed with PBS and fixed in a mixture of 1% formaldehyde and 1% glutaraldehyde in 0.1 M phosphate buffer for about 12 h at 4°C. After washing with buffer, cells were treated with 2% osmium tetroxide and 1.5% potassium ferrocyanide (K<sub>4</sub>[Fe(CN)<sub>6</sub>]) in 0.1 M phosphate buffer for 4 h at room temperature. Several washing steps with the buffer and with water removed non-bound salts before en bloc contrasting in aqueous 2% uranyl acetate for 45 min was performed. Afterwards, the cell layers were washed with water and dehydrated through a series of ethanol (35%, 50%, 75%, 90%, each for 10 min). Infiltration with the epoxy-resin EMBED 812 (EMS, Fort Washington, Pa., USA) was carried out by incubating the cell layers with hydroxypropyl methacrylate (HPMA; 90%, 95%, 97%, each for 15 min) as an intermedium. Subsequently, these treated filters were cut into smaller pieces and further infiltrated with mixtures of HPMA and EMBED (2:1, 1:1, each for 15 min, and 1:2, for 30 min) and pure EMBED (overnight). Finally, filter pieces were embedded in fresh EMBED and polymerised at 60°C.

Ultrathin sections (60–80 nm thick) were cut perpendicular to the filter surface by using an ultramicrotome (Leica, Bensheim, Germany). After staining with uranyl acetate and lead citrate to improve the contrast, sections were observed and photographed in a transmission electron microscope (Zeiss EM10C, Oberkochen, Germany) at 60 or 80 kV.

## Light microscopy

Cell layers were fixed in Bouin's solution on day 18 of culture (when AIC-grown cell layers showed their peak TEER), dehydrated in 2-propanol, and embedded in paraffin. Sections were taken with a steel knife in a rotational microtome (Jung, Heidelberg, Germany) and stained with Nuclear Fast red, eosin Y, aniline blue, and orange G to show nuclei, acidic products, and secretory components, respectively.

## Statistical analysis

Results are expressed as mean $\pm$ SD. Significance ( $P<0.05$ ) of differences in the TEER values were determined by one-way analysis of variances, followed by Neumann-Keuls-Student post-hoc tests.

## Results

### Bioelectrical properties

The gradual development of TEER values for *16HBE14o-* cell layers grown under a variety of LCC and AIC conditions is depicted in Fig. 1. After an initial delay of 3 days, TEER values increased for cells cultured in the presence of an apical fluid lining, reaching values between 500 and 800  $\Omega\cdot\text{cm}^2$  on days 7–8. A maximum of  $791\pm176 \Omega\cdot\text{cm}^2$  ( $n=12$ ) was attained for cells with 250  $\mu\text{l}$  apical and 900  $\mu\text{l}$  basolateral medium (Table 1). Cells cultured with apical/basolateral volumes of 100  $\mu\text{l}/750 \mu\text{l}$ , 750  $\mu\text{l}/1800 \mu\text{l}$ , and 1000  $\mu\text{l}/2100 \mu\text{l}$  showed significantly lower peak TEER values of  $533\pm76 \Omega\cdot\text{cm}^2$ ,  $554\pm14 \Omega\cdot\text{cm}^2$ , and  $542\pm14 \Omega\cdot\text{cm}^2$  ( $n=12$ ), respectively. Cells cultured under standard conditions (500  $\mu\text{l}$  apically, 1500  $\mu\text{l}$  basolaterally) showed a maximum at  $671\pm133 \Omega\cdot\text{cm}^2$  ( $n=60$ ), which was not significantly different from the maximum observed in cells with 250  $\mu\text{l}$  apical culture medium. After the peak on days 7–9, resistance values decreased slowly to values around 400  $\Omega\cdot\text{cm}^2$  by day 14. In contrast, *16HBE14o-* cells under AIC conditions did not develop a peak electrical resistance over a period of 18 days (Fig. 1). TEER values increased slowly to the value of  $127\pm20 \Omega\cdot\text{cm}^2$  ( $n=12$ ) on day 17 with no clear peak appeared. Instead, a steady increase was observed that closely followed the increase in cell number (data not shown).

### Immunofluorescence staining

#### Tight junctions

Staining for ZO-1 in both AIC- and LCC-grown cells was performed after 2 days, 4 days, 1 week, and 2 weeks from seeding (Fig. 2). Cells cultured under AIC or LCC conditions showed some expression of ZO-1 along the cell borders on day 2. However, staining was irregular in pattern, and ZO-1 negative spots were dominant in each case. The cell layers had not yet reached confluency on day 2, as determined by their low TEER values (Fig. 1).

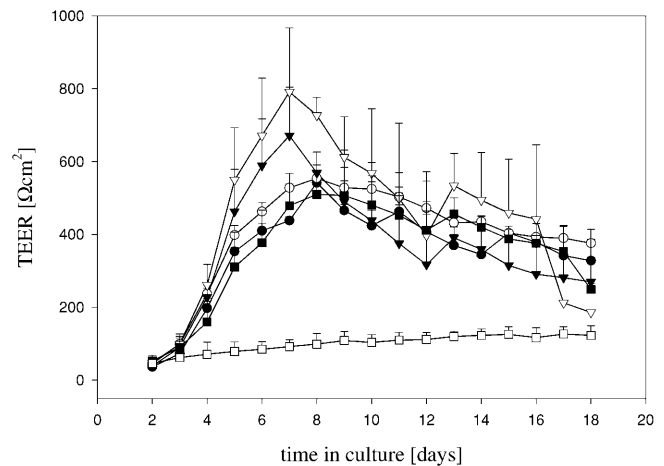


**Fig. 1** Time course of TEER development in *16HBE14o-* cells. Cells were seeded at a density of  $10^5$  cells/ $\text{cm}^2$  on Transwell Clear inserts and cultured with 1000  $\mu\text{l}$  (solid circles), 750  $\mu\text{l}$  (open circles), 500  $\mu\text{l}$  (solid triangles), 250  $\mu\text{l}$  (open triangles), or 100  $\mu\text{l}$  (solid squares) apical medium, or exposed to an air-interface from day 1 (i.e., 24 h post-seeding) onward (open squares). Each data point represents the mean $\pm$ SD ( $n=12$ , except for  $n=60$  for 500  $\mu\text{l}$ ) from three different passages

**Table 1** Maximal TEER values of *16HBE14o-* cell layers grown with various apical fluid volumes ( $n=12$ , except for  $n=60$  for 500  $\mu\text{l}$ )

Volume ( $\mu\text{l}$ )		TEER <sub>max</sub> ( $\Omega\cdot\text{cm}^2$ )	SD
Apical	Basolateral		
0	700	127	$\pm 20$
100	750	533	$\pm 76$
250	900	791	$\pm 176$
500	1500	671	$\pm 133$
750	1800	554	$\pm 14$
1000	2100	542	$\pm 14$

After 4 days in culture, the confluency of the cells increased under both culture conditions. However, ZO-1 staining intensity increased only for LCC-grown cells; this staining appeared to be more regular than that observed in cells on day 2 (Fig. 2). AIC-grown cells had lost most of their ZO-1 expression on day 4 (Fig. 2). After one week from seeding, the ZO-1 staining of AIC-grown cells reappeared but was highly irregular. In contrast, after 1 week, the LCC-grown cells stained very intensely for ZO-1, which was found mostly along intercellular contacts. Two weeks of culturing cells did not change the ZO-1 staining profiles, although it became weaker in LCC-grown cells.

To confirm the presence of tight junctions, AIC- and LCC-grown cells were stained for tight-junctional proteins, occludin (Fig. 3, top) and claudin-1 (Fig. 3, middle), after 1 week in culture (corresponding to peak TEER values). The staining pattern followed that observed for ZO-1, with a regular appearance along the cell borders in LCC-grown cells and an incomplete and irregular appearance in cells grown under AIC conditions.

**Fig. 2** Synthesis of ZO-1 in *16HBE14o-* cell cultures. Cells were seeded at a density of  $10^5$  cells/cm<sup>2</sup> on Transwell Clear inserts and cultured under LCC (*left*) throughout or AIC (*right*) conditions from day 1 onward. Cultured cell layers were fixed after 2 days, 4 days, 1 week, or 2 weeks from seeding and stained for the tight-junctional protein ZO-1 (*green*) as described. Nuclei were counterstained with propidium iodide (*red*). The focal plane lies within the apical-most cell layers. Bars represent  $\mu\text{m}$

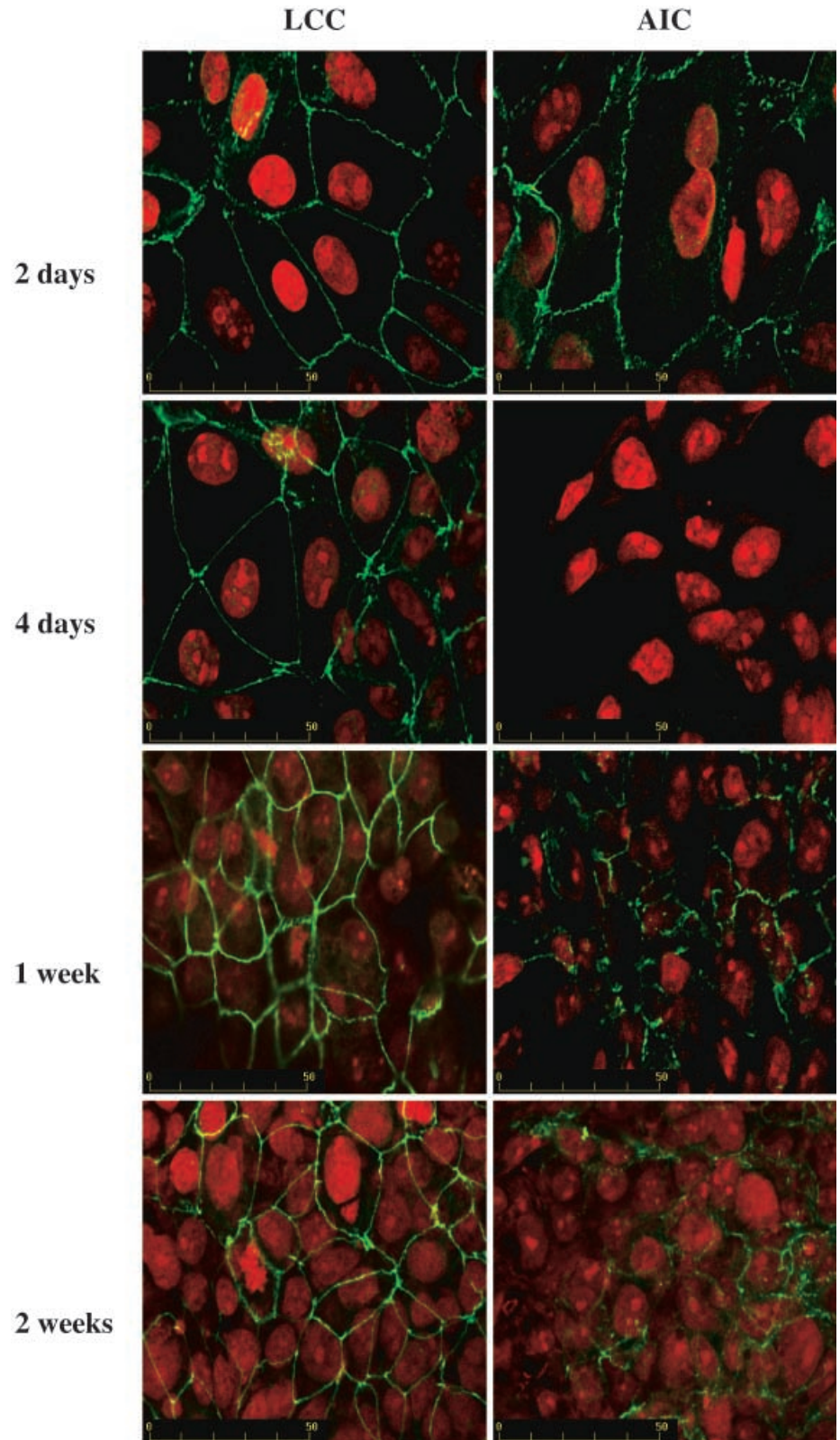
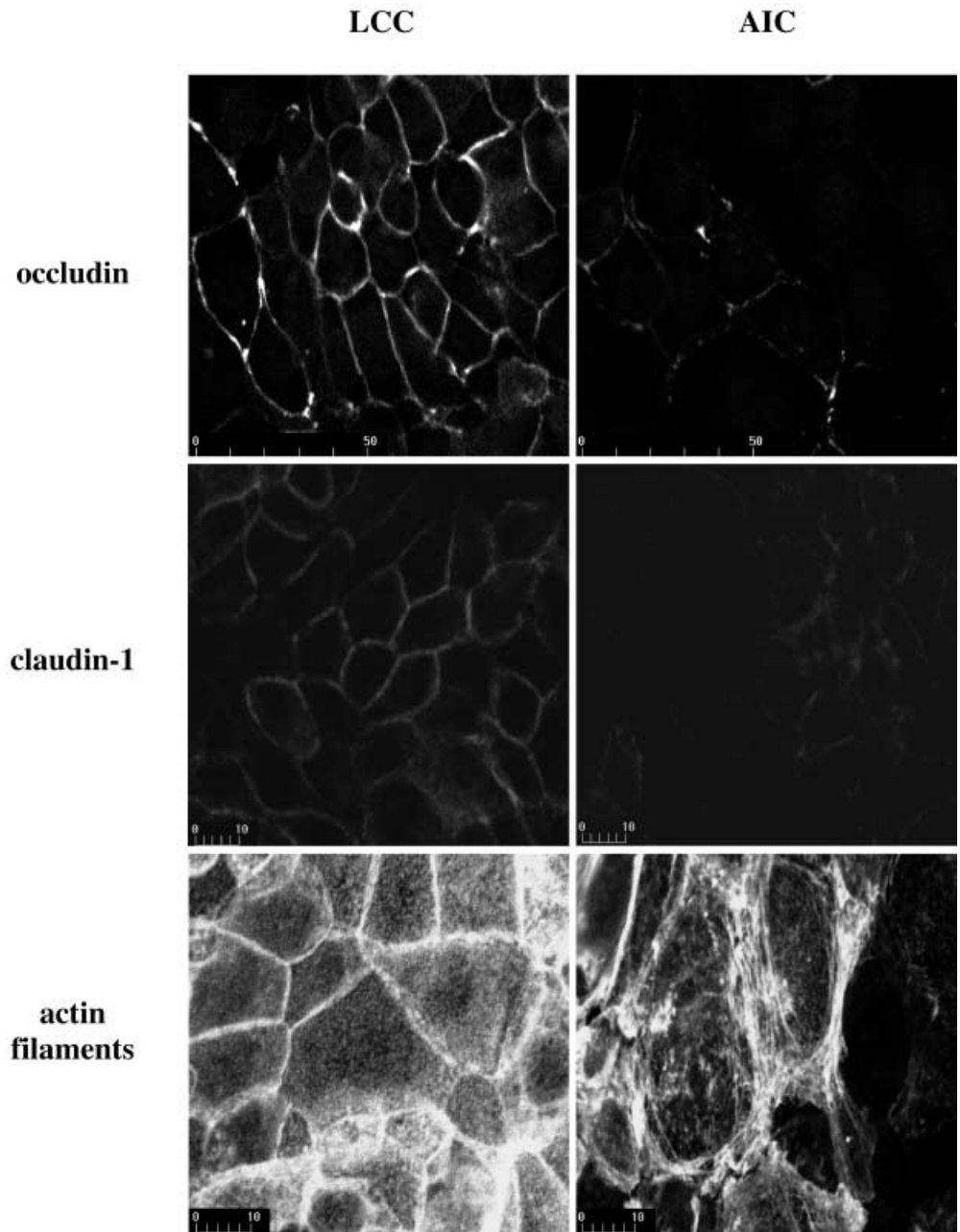


**Fig. 3** Demonstration of occludin, claudin-1, and actin filaments after 1 week of culture of *16HBE14o-* cells. Cells were seeded at a density of  $10^5$  cells/cm<sup>2</sup> on Transwell Clear inserts and grown under LCC (*left*) throughout or AIC (*right*) conditions from day 1 onward. Cultured cell layers were stained on day 7 for occludin, claudin-1, or actin filaments as described. The focal plane lies within the apical-most cell layers. Bars represent  $\mu$ m



#### *Adherens junctions*

Cells grown under either AIC or LCC conditions stained positively for E-cadherin along the intercellular interface (Fig. 4, lower two panels), although the staining was more intense and regular in appearance in LCC-grown cell layers.

#### *Gap junctions*

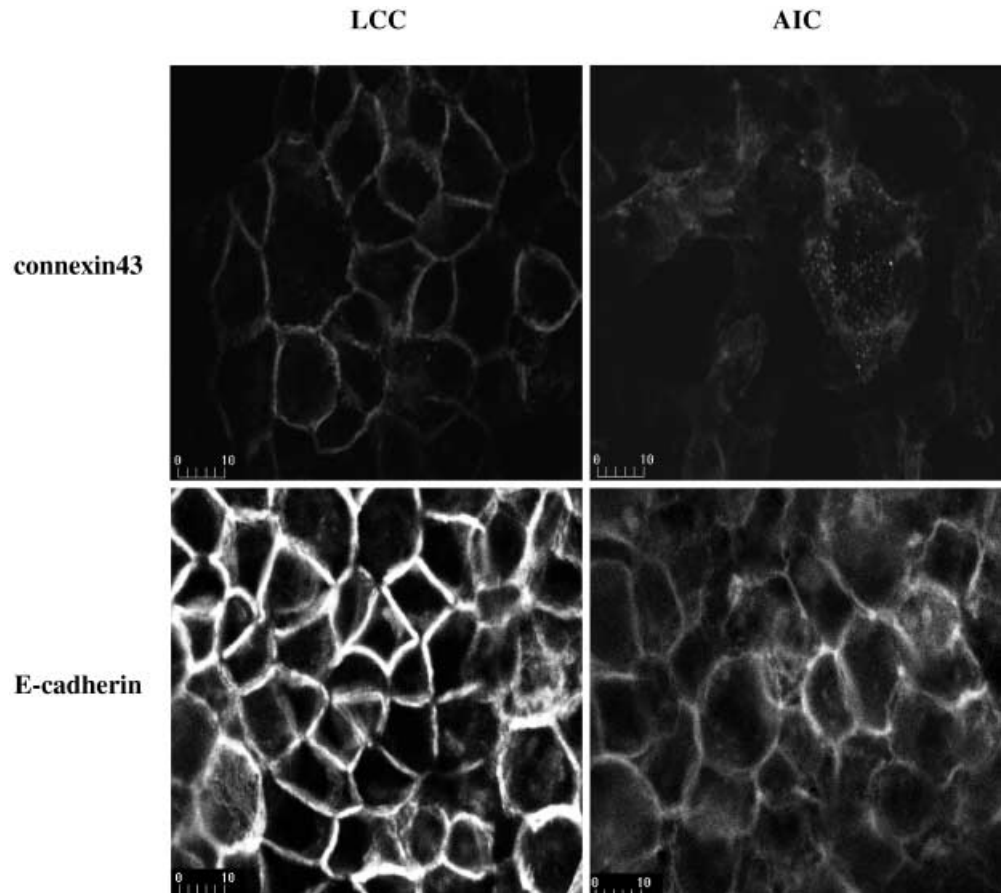
*16HBE14o-* cells maintained under LCC conditions showed positive staining for Cx43 along the cell-cell interface (Fig. 4, upper left panel), whereas staining pro-

files in AIC-grown cells showed a spotty cytoplasmic pattern (Fig. 4, upper right panel).

#### *Actin filaments*

Cell-cell adhesion proteins are linked to cytoskeletal filaments, with the major component being actin. The arrangement of the actin filaments in the *16HBE14o-* cells was visualized by phalloidin labeling. We observed a major difference with regard to the filamental organization between AIC- and LCC-grown cell layers (Fig. 3, bottom panels). Whereas the actin filaments were highly organized immediately underneath the cell membranes

**Fig. 4** Distribution of E-cadherin and connexin43 after 1 week of culture of *16HBE14o-* cells. Cells were seeded at a density of  $10^5$  cells/cm<sup>2</sup> on Transwell Clear inserts and grown under LCC (*left*) throughout or AIC (*right*) conditions from day 1 onward. Cultured cell layers were stained on day 7 for connexin43 or E-cadherin as described. The focal plane lies within the apical-most cell layers. Bars represent  $\mu$ m



and extended to the cellular junction under LCC conditions, they appeared irregular in pattern in AIC-grown cells and resembled those seen in cells that grow in isolation (i.e., with no cell-cell contact). The image shown for LCC-grown cells (Fig. 3, left bottom panel) demonstrates the presence of microvilli, which appear as small dots, on the cell surface.

#### Electron microscopy

Cells grown under LCC conditions formed a multilayer of up to 5 cells in thickness. Contact structures between cells were well developed. Cells in the apical most surface layer were connected by tight junctions and adherens junctions (Fig. 5). Cells maintained with an air-interface grew as a cell layer up to 16 cells in thickness, and the tight junctions showed a highly irregular appearance (data not shown). Microvilli were formed under both culture conditions.

**Fig. 5** Transmission-electron micrograph of *16HBE14o-* cells grown on Clearwells under LCC conditions for 1 week. Apical cell-cell contacts consist of tight junctions (*tj*) and adherens junctions (*aj*) between two cells. The apical plasma membrane possesses several microvilli (*mv*). Bar 0.2  $\mu$ m

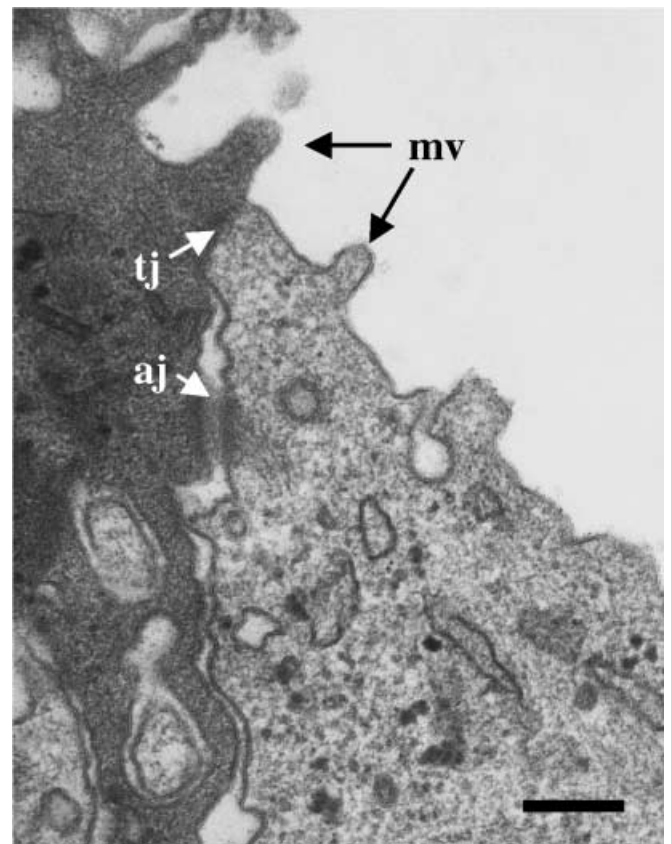


**Table 2**  $P_{app}$  values and recovery balances of drugs and permeation markers across cell layers of *16HBE14o-* cells

Solutes	MW in Daltons	$P_{app}$ ( $\times 10^{-6}$ cm $\cdot$ s $^{-1}$ ) <sup>a</sup>		Recovery (%)	
		LCC	AIC	LCC	AIC
Fluorescein-Na	376	0.85 $\pm$ 0.03	4.90 $\pm$ 0.54*	99	101
FITC-dextran 4000	4400	0.42 $\pm$ 0.12	1.53 $\pm$ 0.18*	105	104
Atenolol	266	3.87 $\pm$ 0.11	7.18 $\pm$ 0.56*	103	101
Propranolol HCl	296	26.60 $\pm$ 1.68	15.93 $\pm$ 4.74*	86	74

<sup>a</sup> Mean $\pm$ SD ( $n=12$ )

\*Significantly different from that observed for LCC-grown cell layers

### Paracellular integrity

To assess the paracellular permeability of *16HBE14o-* cells, transport experiments with the anionic hydrophilic marker, Flu-Na, were performed on consecutive days in culture. In general,  $P_{app}$  for Flu-Na decreased with increasing TEER values (Fig. 6). No significant decreases in  $P_{app}$  were observed for cell layers with TEER values higher than 270  $\Omega\cdot$ cm $^2$ . However, this value could only be reached with cell layers grown under LCC conditions. The minimum paracellular permeability for Flu-Na was 0.85 $\pm$ 0.03 $\times 10^{-6}$  cm $\cdot$ sec $^{-1}$ . AIC-grown cells did not develop TEER values higher than 127 $\pm$ 19  $\Omega\cdot$ cm $^2$ . The  $P_{app}$  for Flu-Na at this TEER was 4.90 $\pm$ 0.54 $\times 10^{-6}$  cm $\cdot$ sec $^{-1}$ .

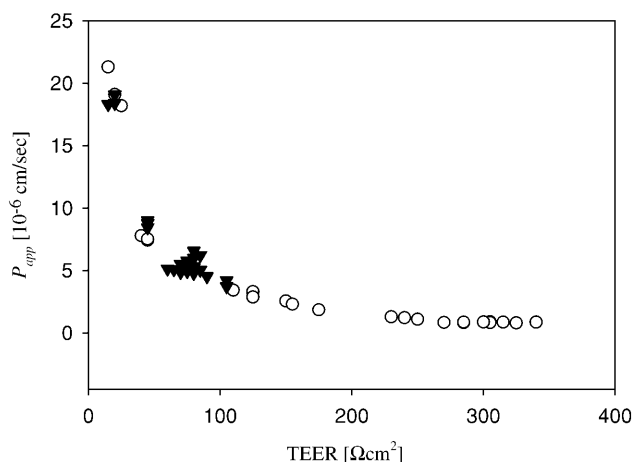
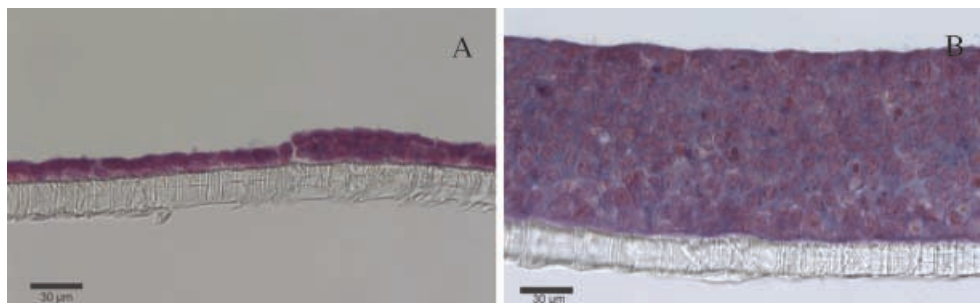


**Fig. 6** Correlation between the apparent permeability ( $P_{app}$  for Flu-Na) of cell layers and TEER. *16HBE14o-* cells were seeded at a density of  $10^5$  cells/cm $^2$  on Transwell Clear inserts and maintained under LCC (open circles) or AIC (solid triangles) conditions from day 1.

**Fig. 7A, B** Light micrograph of *16HBE14o-* cells after 18 days in culture. Cells were seeded at a density of  $10^5$  cells/cm $^2$  on Transwell Clear inserts and cultured under LCC (A) throughout or AIC (B) conditions from day 1 onward



The curve for Flu-Na  $P_{app}$  vs. TEER for LCC-grown cell layers with TEER of less than 100  $\Omega\cdot$ cm $^2$  approximated that for AIC-grown cells, indicating a common (e.g., passive diffusional) process being responsible for Flu-Na translocation across cells under both types of culture conditions.

The  $P_{app}$  values for FD4 and the BCS marker drugs are summarized in Table 2. For the hydrophilic substances (Ate and FD4), the  $P_{app}$  values were higher for AIC- than LCC-grown cells, indicating the leakiness of the cell layer. For the lipophilic Pro, the opposite was found. The fluxes for Pro across LCC-grown *16HBE14o-* cell layers were faster than those across AIC-grown cells. The amount of recovered drug (balance of samples and remaining drug in the donor compartment) after the experiment was approximately 100% for the hydrophilic drugs. For Pro, it was 86% and 74% for the LCC- and AIC-grown cell layers, respectively.

### Light microscopy

LCC-grown *16HBE14o-* cell layers formed an epithelial barrier consisting of 1–5 cells (Fig. 7A), compared with layers of 10–16 cells under AIC conditions (Fig. 7B). The LCC-grown cell layers showed a more flattened morphology, whereas under AIC conditions, cells appeared more rounded (i.e., displaying squamous metaplasia).

### Discussion

In the present study, we have critically evaluated the influence of AIC vs LCC conditions on the morphology and functional properties of the human bronchial epithelial cell line, *16HBE14o-*, as a polarized cell layer with

cellular contacts. When grown under LCC conditions, *16HBE14o-* cells form layers with a height of 1-5 cells, comparable with bronchial epithelium *in vivo*. As visualized by immunofluorescence staining and electron microscopy, these cell layers form well-defined tight, adherens, and gap junctions, and highly organized actin filaments. These results are accompanied by high TEER values (up to  $\sim 800 \Omega\text{-cm}^2$ ). The permeability of marker drugs and substances across the LCC-grown human bronchial epithelial cell layers is comparable to those data obtained in our laboratory under the same conditions with *Caco-2* monolayers (data not shown).

In contrast, when grown at an air-interface, *16HBE14o-* cells display no clear polar organization and form cell layers of 10–16 cells in thickness with a morphology associated with squamous metaplasia. Despite their thickness, these cell layers do not develop TEER values greater than  $130 \Omega\text{-cm}^2$ . Cellular contacts form very poorly, and the actin filaments of *16HBE14o-* cells grown under AIC conditions show characteristics similar to cells growing separated from each other (Hamm-Alvarez et al. 2001). Additionally, drug absorption studies have shown that AIC-grown cell layers do not possess a functional barrier to solutes. The highly lipophilic drug Pro diffuses much more slowly across cell layers maintained at an air-interface, as compared with cell layers grown under LCC conditions. A possible explanation for this finding might be the greater drug quantity accumulated inside the AIC-grown cells, as can be gauged from the lower recovery balance, because of their greater number.

Conflicting reports concerning the air-interfaced culture of cells derived from respiratory tissues are available to date. For example, Yamaya et al. (1992) have demonstrated that the differentiation of human tracheal epithelial cells in culture is inversely correlated to the depth of liquid overlying the apical surface of the cells. By contrast, de Jong and coworkers (1993) have reported that human bronchial epithelial cells (derived from biopsies and subcultured for up to 8 passages) form 3–6 layers of cells exhibiting squamous metaplasia under AIC conditions, whereas LCC conditions lead to maximally 3 layers of polygon-shaped, small cuboidal cells with an appearance resembling basal cells *in vivo*, similar to our current findings.

The mechanisms underlying the way in which AIC conditions influence cell differentiation at the molecular level are yet to be unraveled. Many parameters must be taken into consideration, including the concentration of nutrients and the presence of serum on the apical side, the developing pH gradient attributable to altered  $\text{CO}_2$  passage, or the influence of surfactant/mucus lining. *16HBE14o-* cells display many properties of bronchial basal cells. They show the same lectin-binding patterns (Dorscheid et al. 1999) and express ICAM-1 (Zhu et al. 1999) as basal cells do. Additionally, they produce no secretory component (Godding et al. 1998).

It is possible that a collapse of  $\text{Na}^+/\text{H}^+$  gradients results in a breakdown of connexin43 trafficking (de Sousa

et al. 1993), leading to poor development of cell-cell junctions. Alteration of the GJIC could be the trigger for the cancer-like proliferation observed for AIC-grown *16HBE14o-* cells (Jinn et al. 1998; Ruch et al. 2001). The apical fluid lining present under LCC conditions may substitute for the mucus found on bronchial cells *in vivo*, allowing the cells to develop normally.

In summary, the *16HBE14o-* cell line grown under LCC conditions appears to be a useful model for mechanistic studies of the regulation of bronchial epithelial cell function and the effects of various culture conditions on cell signaling, proliferation, and differentiation at cellular and molecular levels. Moreover, this *in vitro* model allows us rapidly to screen novel drug candidates and formulations targeted for systemic absorption via the airways or local action on the respiratory epithelium.

**Acknowledgements** We thank Dr. Dieter C. Gruenert, San Francisco, Calif., USA, for the generous gift of the *16HBE14o-* cell line, Dr. Michael Laue, Department of Anatomy, Saarland University, Homburg, Germany, for his microscopical and histological expertise, and Ms. Isabell Erler, Ms. Jeannette Möbius, and Mr. Roland Fuchs for their skillful technical assistance.

## References

- Abraham V, Chou ML, George P, Pooler P, Zaman A, Savani RC, Koval M (2001) Heterocellular gap junctional communication between alveolar epithelial cells. *Am J Physiol* 280:L1085–L1093
- Amidon GL, Lennernas H, Shah VP, Crison JR (1995) A theoretical basis for a biopharmaceutical drug classification: the correlation of *in vitro* drug product dissolution and *in vivo* bioavailability. *Pharm Res* 12:413–420
- Aoki Y, Qiu D, Zhao GH, Kao PN (1998) Leukotriene  $\text{B}_4$  mediates histamine induction of NF- $\kappa\text{B}$  and IL-8 in human bronchial epithelial cells. *Am J Physiol* 274:L1030–L1039
- Artursson P (1990) Epithelial transport of drugs in cell culture. I: A model for studying the passive diffusion of drugs over intestinal absorptive (*Caco-2*) cells. *J Pharm Sci* 79:476–482
- Bonvallot V, Baeza-Squiban A, Baulig A, Brulant S, Boland S, Muzeau F, Barouki R, Marano F (2001) Organic compounds from diesel exhaust particles elicit a proinflammatory response in human airway epithelial cells and induce cytochrome p450 1A1 expression. *Am J Respir Cell Mol Biol* 25:515–521
- Cheek JM, Kim KJ, Crandall ED (1989) Tight monolayers of rat alveolar epithelial cells: bioelectric properties and active sodium transport. *Am J Physiol* 256:C688–C693
- Cozens AL, Yezzi MJ, Yamaya M, Steiger D, Wagner JA, Garber SS, Chin, Simon EM, Cutting GR, Gardner P, Friend DS, Basbaum CB, Gruenert DC (1992) A transformed human epithelial cell line that retains tight junctions post crisis. *In Vitro Cell Dev Biol* 28A:735–744
- Cozens AL, Yezzi MJ, Kunzelmann K, Ohru T, Chin L, Eng K, Finkbeiner WE, Widdicombe JH, Gruenert DC (1994) CFTR expression and chloride secretion in polarized immortal human bronchial epithelial cells. *Am J Respir Cell Mol Biol* 10:38–47
- Dobbs LG (1990) Isolation and culture of alveolar type II cells. *Am J Physiol* 258:L134–L147
- Dorscheid DR, Conforti AE, Hamann KJ, Rabe KF, White SR (1999) Characterization of cell surface lectin-binding patterns of human airway epithelium. *Histochem J* 31:145–151
- Elbert KJ, Schäfer UF, Schäfers HJ, Kim KJ, Lee VHL, Lehr CM (1999) Monolayers of human alveolar epithelial cells in primary culture for pulmonary absorption and transport studies. *Pharm Res* 16:601–608

- Fanning AS, Jameson BJ, Jesaitis LA, Anderson JM (1998) The tight junction protein ZO-1 establishes a link between the transmembrane protein occludin and the actin cytoskeleton. *J Biol Chem* 273:29745–29753
- Furuse M, Itoh M, Hirase T, Nagafuchi A, Yonemura S, Tsukita S (1994) Direct association of occludin with ZO-1 and its possible involvement in the localization of occludin at tight junctions. *Am J Physiol* 274:F1–F9
- Furuse M, Fujita K, Hிராги T, Fujimoto K, Tsukita S (1998) Claudin-1 and -2: novel integral membrane proteins localizing at tight junctions with no sequence similarity to occludin. *J Cell Biol* 141:1539–1550
- Godding V, Sibille Y, Massion PP, Delos M, Sibille C, Thurion P, Giffroy D, Langendries A, Vaerman JP (1998) Secretory component production by human bronchial epithelial cells is up-regulated by interferon gamma. *Eur Respir J* 11:1043–1052
- Hamm-Alvarez SF, Chang A, Wang Y, Jerdeva G, Lin HH, Kim KJ, Ann DK (2001) Etk/Bmx activation modulates barrier function in epithelial cells. *Am J Physiol* 280:C1657–C1668
- Hodge S, Hodge G, Holmes M, Flower R, Scicchitano R (2001) Interleukin-4 and tumor necrosis factor- $\alpha$  inhibit transforming growth factor- $\beta$  production in a human bronchial epithelial cell line: possible relevance to inflammatory mechanisms in chronic obstructive pulmonary disease. *Respirology* 6:205–211
- Itoh M, Furuse M, Kazumasa M, Kubota K, Saitou M, Tsukita S (1999) Direct binding of three tight junction-associated MAGUKs, ZO-1, ZO-2, and ZO-3, with the COOH termini of claudins. *J Cell Biol* 147:1351–1363
- Jinn Y, Ichioka M, Marumo F (1998) Expression of connexin32 and connexin43 gap junction proteins and E-cadherin in human lung cancer. *Cancer Lett* 127:161–169
- Jong PM de, Sterkenburg MAJA van, Kempenaar JA, Dijkman JH, Ponc M (1993) Serial culturing of human bronchial epithelial cells derived from biopsies. *In Vitro Cell Dev Biol* 29A:379–387
- Lampe PD, Lau AF (2000) Regulation of gap junctions by phosphorylation of connexins. *Arch Biochem Biophys* 384:205–215
- Madara JL (1987) Intestinal absorptive cell tight junctions are linked to cytoskeleton. *Am J Physiol* 253:C171–C175
- Mak VH, Cumpstone MB, Kennedy AH, Harmon CS, Guy RH, Potts RO (1991) Barrier function of human keratinocyte cultures grown at the air-liquid interface. *J Invest Dermatol* 96:323–327
- Man Y, Hart VJ, Ring CJA, Sanjar S, West MR (2000) Loss of epithelial integrity resulting from E-cadherin dysfunction predisposes airway epithelial cells to adenoviral infection. *Am J Respir Cell Mol Biol* 23:610–617
- Mathias NR, Kim KJ, Robison TW, Lee VHL (1995) Development and characterization of rabbit tracheal epithelial cell monolayer models for drug transport studies. *Pharm Res* 12:1499–1505
- Mitic LL, Anderson JM (1998) Molecular architecture of tight junctions. *Annu Rev Physiol* 60:121–142
- Morita K, Furuse M, Fujimoto K, Tsukita S (1999) Claudin multi-gene family encoding four-transmembrane domain protein components of tight junction strands. *Proc Natl Acad Sci* 96:511–516
- Polosa R, Prosperini G, Leir SH, Holgate ST, Lackie PM, Davies DE (1999) Expression of c-erbB receptors and ligands in human bronchial mucosa. *Am J Respir Cell Mol Biol* 20:914–923
- Ruch RJ, Porter S, Koffler LD, Dwyer-Nield LD, Malkinson AM (2001) Defective gap junctional intercellular communication in lung cancer: loss of an important mediator of tissue homeostasis and phenotypic regulation. *Exp Lung Res* 27:231–243
- Salvi S, Semper A, Blomberg A, Holloway J, Jaffar Z, Papi A, Teran L, Polosa R, Sandström T, Holgate ST, Frew A (1999) Interleukin-5 production by human airway epithelial cells. *Am J Respir Cell Mol Biol* 20:984–991
- Shen BQ, Finkbeiner WE, Wine JJ, Mrsny RJ, Widdicombe JH (1994) *Calu-3*: a human airway epithelial cell line that shows cAMP-dependent Cl<sup>-</sup> secretion. *Am J Physiol* 266:L493–L501
- Shen J, Elbert KJ, Yamashita F, Lehr CM, Kim KJ, Lee VHL (1999) Organic cation transport in rabbit alveolar epithelial cell monolayers. *Pharm Res* 16:1280–1287
- Simon AM, Goodenough DA (1998) Diverse functions of vertebrate gap junctions. *Trends Cell Biol* 8:477–482
- Simon DB, Lu Y, Choate KA, Velazquez H, Al-Sabban E, Praga M, Casari G, Bettinelli A, Colussi G, Rodriguez-Soriano J, McCredie D, Milford D, Sanjad S, Lifton RP (1999) Paracellin-1, a renal tight junction protein required for paracellular Mg<sup>2+</sup> resorption. *Science* 285:103–106
- Sousa PA de, Valdimarsson G, Nicholson BJ, Kidder GM (1993) Connexin trafficking and the control of gap junction assembly in mouse preimplantation embryos. *Development* 117:1355–1367
- Yamaya M, Finkbeiner WE, Chun SY, Widdicombe JH (1992) Differentiated structure and function of cultures from human tracheal epithelium. *Am J Physiol* 262:L713–L724
- Yang JJ, Ueda H, Kim KJ, Lee VHL (2000) Meeting future challenges in topical ocular drug delivery: development of an air-liquid primary culture of rabbit conjunctival epithelial cells on a permeable support for drug transport studies. *J Control Release* 65:1–11
- Zhu J, Rogers AV, Burke-Gaffney A, Helleweg PG, Jeffery PK (1999) Cytokine-induced airway epithelial ICAM-1 upregulation: quantification by high-resolution scanning and transmission electron microscopy. *Eur Respir J* 13:1318–1328